Multimed Tools Appl (2018) 77:21923–21933
https://doi.org/10.1007/s11042-017-5362-x

Approach to weak signal detection via over-sampling and bidirectional saw-tooth shaped function in wearable devices

Enmin Song[1] · **Ning Cheng**[1] · **Hong Liu**[1] · **Huimin Song**[2]

Received: 7 June 2017 / Revised: 8 September 2017 / Accepted: 25 October 2017 /
Published online: 11 November 2017

Abstract Many biological signals that reflect the human health are relatively weak, and high-resolution Analog-Digital Converters (ADCs) are required to measure them. The over-sampling technology is a method for increasing the accuracy, equal to the accuracy of high resolution ADCs, when an ADC has low resolution. For high resolution ADCs, their accuracy from the over-sampling technology would break its maximum limitation. During our signal collection, there are two items which affect our results: 1. measurement error; 2. non-linear characteristics at the end points. In over-sampling method of detecting weak signal of wearable devices by using the unidirectional saw-tooth shaped function, the magnitude of the shaped function is as close as possible to the integer multiple of the quantization step size to reduce the additional measurement error. To reduce the difficulty of the adding shaped function, which features nonlinearity of the starting point, a new method of detecting the weak signal by adding the bidirectional saw-tooth shaped function is proposed. The experimental results show this method is feasible for improving the ADC resolution.

Keywords Weak signal detection · Bidirectional saw-tooth shaped function · Over-sampling · Nonlinearity of the starting point

✉ Hong Liu
hongliu@hust.edu.cn

Enmin Song
esong@hust.edu.cn

Ning Cheng
cning@hust.edu.cn

Huimin Song
allen@centralcitybrewing.com

[1] School of Computer Science and Technology, Huazhong University of Science and Technology, Wuhan 430074, China

[2] Central City Brewers and Distillers, 11411 Bridgeview Drive, Surrey, BC V3R0C2, Canada

1 Introduction

In recent years, with the continuous improvement of quality of life, people pay more attention to physical health and want to have a further understanding of their own physical health. Many scholars did substantive research in the field of healthcare [1, 2, 10–12]. Many indexes are used to reflect health conditions, including blood pressure, heart rate and body temperature. These indexes can be measured by a few simple medical devices which ordinary families can easily purchase, and their prices are relatively cheap. Other indexes of health, such as blood glucose, blood oxygen saturation, total cholesterol, and lipids are more important in some cases, but they can be harder to measure. Firstly, people may have to go to the hospital or designated medical laboratories for data collection. Secondly, the prices of these equipment are more expensive. Thirdly, continuous travelling between the family and medical institutions cost energy and financial resources. The above inconveniences prevent people from satisfying their concern about physical health. Fortunately, with the development of various micro-sensors, measurement equipment with smaller size and lower price, and wearable measuring equipment are coming into being. However, current portable instruments may not have the same accuracy as the medical equipment in hospitals. For example, portable blood glucose meters measure the blood glucose concentration of the whole blood, whereas blood glucose meters in hospitals measure glucose concentration of plasma after filtering blood cells. Yet, portable instruments have had guiding significance to common people.

Among these health indexes, the blood glucose concentration is frequently measured. At present, there are many portable blood glucose meters in the market, but they have disadvantages. For instance, data collection requires blood samples and result accuracy relies on fasting blood glucose and postprandial blood glucose. In this case, the result from one-time measurements may be highly random. However, measurements, collected over a period, carried out at the same time every day, would be stable and useful. For the sake of improving people's adherence, reducing the discomfort of each blood collection, and increasing analyzability of the measurement results, the continuous dynamic blood glucose meter was invented. The various signals that reflect the health of the human body are analog signals, and they are shown on the electronic device, using ADC (Analog-Digital Convertor). Due to volume constraints, a dynamic blood glucose meter cannot work with a large power supply system and large-size chips. This increases the difficulties of measuring the weak signals.

A weak signal has two meanings: 1. the strength of the signal itself is very weak; 2. the strength of the signal itself is not weak but its fluctuation within a short time is very small. The blood glucose level has small fluctuations in seconds, so a high-resolution ADC is required to measure such signal.

The wireless dynamic blood glucose monitoring system is a new type of instrument, which is used to collect weak signals of body fluid current in real time, via implanting a glucose sensor under the skin. The signals are amplified and transformed to the receiver end [3]. Figure 1 shows an ADC unit in the wireless acquisition system.

If a 24-bit ADC (for example AD7787 [8]) is used in the system, it will achieve a high measurement accuracy, but its cost will be high as well. In general, a higher resolution ADC has higher sensitivity to noise even the reference voltage is the same. For the measurement using a lower resolution ADC, the weak signal needs to be amplified and filtered to improve their measurement accuracy. The over-sampling technique allows the low-resolution ADCs to detect weak signals without the use of an amplifier circuit, which can also make high-resolution ADCs break their highest resolution. Over-sampling technology is a common

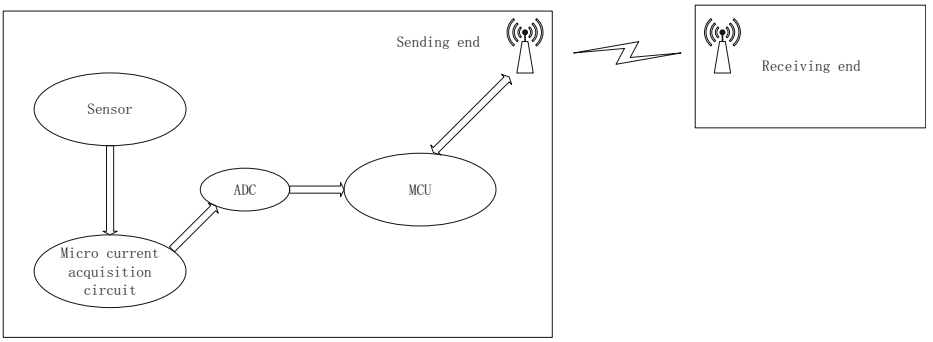

Fig. 1 Wireless acquisition system

method to improve the resolution of measurement and control system, which has been widely used in various fields [4, 6, 7, 9].

2 Adding saw-tooth shaped function

In this section, we introduce the relationship between ADC and over-sampling technique, and some problems we may encounter when using shaped functions.

2.1 Over-sampling technology

When the quantization step size of the ADC is greater than the signal amplitude after superposing the shaped function, the over-sampling technique will fail. Under such circumstances, the readings of the ADC will not be affected, regardless of the total number of samples. To make ADCs read the numeric normally, the magnitude of the shaped function needs to be greater than one quantization step size of the ADC. In addition, it is also necessary to ensure that the signal amplitude does not exceed the input range of the ADC after the addition of the shaped function. When these two conditions are met, the over-sampling technique can work effectively. In other words, first, the shaped signal is modulated to the weak signal and is sampled, and then mixed signal is demodulated into the original signal by calculating high-precision superposed signal with over-sampling technology. To facilitate demodulation after over-sampling, the linear function like saw-tooth wave is often chosen [5].

2.2 The nonlinearity of the shaped function and its influence

When the closed-loop control with negative feedback is applied to the physical components of the signal generator, the circuit is in an unstable state if the feedback signal and the control signal are not balanced. It needs to take a while to enter the steady state. In this case, the added shaped function exhibits significant nonlinearity at the beginning, and the span of the nonlinear interval is related to the device itself. In general, this nonlinear time does not last long.

Ideally, the amplitude range of the superimposed saw-tooth wave is set to start from zero. However, due to the nonlinear effects of the starting point, this kind of the ADC sampling signal is not reliable, so it should be removed. Otherwise, these non-linear sampling data will affect the subsequent calculation of the ADC resolution.

2.3 Parameter setting

We define the voltage value of the measured weak signal s is V_s, the resolution of the ADC is n bits, the reference voltage is V_{REF} and the corresponding analog voltage of a quantization step size is 1LSB.The amplitude of the weak signal is$(S+\Delta S)$LSB, S is a nonnegative integer, $0 \leq \Delta S < 1$. The shaped function STW is a periodic bidirectional saw-tooth wave function, the amplitude is $C_0 = (N+\Delta N)\text{LSB}(N \geq 4, 0 \leq \Delta N < 1)$, and the period is T. Set the sampling frequency is fs, the saw-tooth wave samples m points on average in each LSB.

2.4 Influence of starting-point nonlinearity on unidirectional saw-tooth shaped function

After the signal s is modulated on the STW, the mixed signal S_i is obtained, and then the signal $\bar{s}$ is obtained by rounding down [5]. When the end of the nonlinear effect of starting point is before the first acquisition of the signal amplitude $(x+1)$LSB, the formula given in paper [5] is shown as (M is the number of sampling points of unidirectional saw-tooth waves in one period)

$$\begin{aligned}\bar{s} &= \frac{1}{\mathrm{M}}\sum_{k=1}^{M} S_i \\ &= [(1-\Delta x)mx + (x+1)m + (x+2)m + \cdots + (\Delta x + \Delta x)m(x+N)]/(N+\Delta N)m \quad (1)\end{aligned}$$

The coefficient $(1-\Delta x)m$ in the expansion of Eq.(1) will be affected by the nonlinear effect of the starting point, and sampling frequency of m cannot be calculated or measured. When nonlinear effect of the starting point ends after the first acquisition of the signal amplitude $(x+1)$LSB, both coefficients $(1-\Delta x)m$ and $(x+1)m$ will be affected by nonlinear effect of starting point, which will eventually lead to the inaccurate calculation for the formula.

3 Adding bidirectional saw-tooth shaped function

3.1 Ideal Bidirectional Saw-Tooth Waves

For the same function signal generator, in the case of the same parameters, it can be considered that the duration of nonlinear effect is the same at starting points in each period.

Figure 2 Assuming that the saw-tooth wave is ideal and the waveform start points are not distorted. t_1 is the starting time of the forward saw-tooth wave, t_3 is the starting time of the reverse saw-tooth wave, t_2 is the time point for the sampling results of the ADC from S to S + 1, t_4 is the time point for the sampling results of the ADC from S to S-1

Note that $\Delta ABC \sim \Delta DEF$, Eq.(2) is derived.

$$\frac{\mathrm{DF}}{\mathrm{AC}+\mathrm{DF}} = \frac{\mathrm{EF}}{\mathrm{BC}+\mathrm{EF}} \quad (2)$$

Here, AC represents the sampling time of t_1 to t_2, and DF represents the sampling time of t_3 to t_4. By the definition of LSB, Eq.(3) is derived.

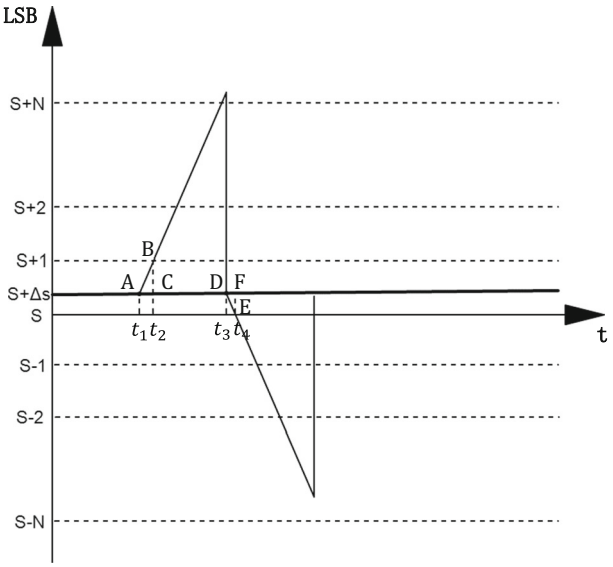

Fig. 2 Ideally bidirectional saw-tooth

$$\mathrm{BC} + \mathrm{EF} = 1\mathrm{LSB} \tag{3}$$

Set from t_1 to t_2 a total of P signals, whose amplitude is SLSB, is collected, and from t_3 to t_4, a total of Q signals, whose amplitude is SLSB, is collected. Eq.(4) is derived.

$$AC = \frac{P}{fs}, DF = \frac{Q}{fs} \tag{4}$$

Substitute Eq.(2) and Eq.(3) into Eq.(4), the sampled value of the ADC developed to $EF = \frac{Q}{P+Q} = \frac{Q}{P+Q}$. The resolution is promoted with $\frac{1}{m}$. The improvement of resolution bit can be estimated by direct oversampling to improve the resolution method, which is shown as $(10lgm)/6.02$ [5].

3.2 Bidirectional saw-tooth waves sampling method with starting point nonlinearity

Since the nonlinear duration of the starting point is unknown and the amplitude of the forward (or reverse) saw-tooth wave in each period is nonlinear at the beginning time, it is possible to cause inaccurate readings of the ADC superposing the forward (or reverse) saw-tooth wave. As shown in Fig. 3, the impact of starting point nonlinearity continues to the end of the time t_2, the sampling results of $t_1 - t_2$ will be influenced.

As shown in Fig. 3, the first time to collect the signal amplitude as S + 2 is set to t_3, the last time to collect the signal amplitude as S + 2 is set to t_4. The first time to collect the signal amplitude as S-2 is set to t_7, the last time to collect the signal amplitude as S-2 is set to t_8. To eliminate the influence of the starting point nonlinearity, the forward saw-tooth wave only counts the sampling data during the period t_3 to t_4, and the reverse saw-tooth only counts the data during the period t_7 to t_8.

The stabilized rising edge of forward saw-tooth wave is set to l_1, and the intersection of signal s is set to O. The stabilized falling edge of reverse saw-tooth is set to l_2. By calculating

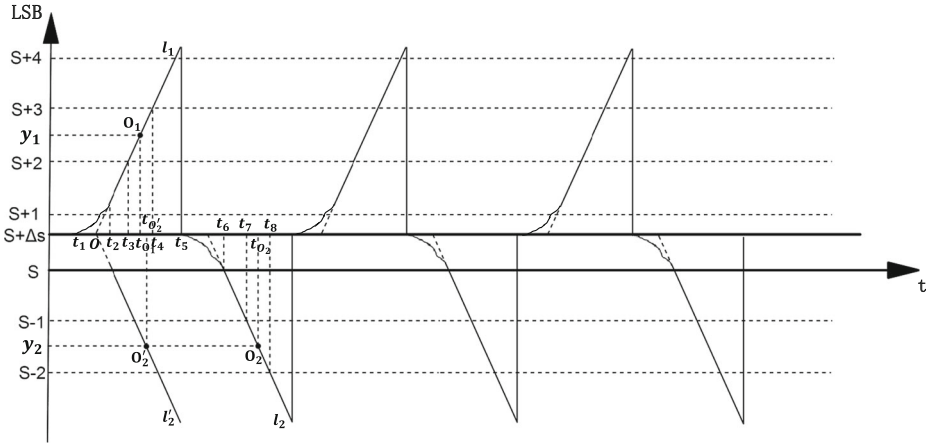

Fig. 3 Bidirectional saw-tooth waves with starting point nonlinearity

the collected signal's mid-time-point t_{O_1} between t_3 and t_4, and making a vertical line to s through the point t_{O_1}, the foot point is O_1, the coordinate is (t_{O_1}, y_1). It's easy to show that $y_1 = S + 2.5$. By calculating the collected signal mid-time-point t_{O_2} between t_7 and t_8, and making a vertical line to s through the point t_{O_2}, the foot point is O_2, the coordinate is (t_{O_2}, y_2). It's easy to show that $y_2 = S - 1.5$. Transforming l_2 and O_2 to the left by T/2, it gets l_2' and O_2', and the coordinate of O_2' is $\left(t_{O_2'}, y_2\right)$. Making a vertical line to s through the point O_2', the foot point is $t_{O_2'}$. The ordinate of the intersection O of l_1 and l_2 is the calculated value of s denoted as s'. Set $\left|t_{O_2'} - t_{O_1}\right| = \varepsilon$. If $\varepsilon = 0$, then $\Delta S = {}^1/_2$LSB. If $\varepsilon > 0$, then Eq.(5) is derived.

$$\frac{t_{O_1} - t_O}{t_{O_2'} - t_O} = \frac{y_1 - s'}{s' - y_2} \tag{5}$$

By the definition of slope, the slope of l_1 can be expressed as

$$k = \frac{2 - (s' - S)}{t_3 - t_O} = \frac{3 - (s' - S)}{t_4 - t_O} \tag{6}$$

According to Eq.(5) and Eq.(6), the results of s' and t_O are derived. Then, the calculated voltage value V_s' of the original signal V_s is shown as

$$V_s' = \frac{V_{REF}}{2^n} \times s' \tag{7}$$

4 Experimental results

An 8-bit ADC is used in this experiment with its reference voltage at 2.533v. In consideration of the limitation of performance of wearable equipment, the sample frequency of ADC is set at 10 Hz, the period of bidirectional shaped saw-tooth function is set at 40s, and its amplitude is 0.16v. According to the definition of m, m = 24.95 is calculated. In order to reduce the random noise, the experiment uses down-sampling technology, that is, the average value of each

Table 1 Experimental results

V_s(v)	Period	Readings of the ADC	V_{ADC}(v)	t_3(ms)	t_4(ms)	t_7(ms)	t_8(ms)	s'	V'_s(v)	Error between V_s and V_{ADC}	Error between V_s and V'_s
1.137	1	114	1.1324	5192	8334	26444	28479	114.6112	1.1385	0.0046	-0.0015
	2	114	1.1324	46692	49032	66228	68670	114.4118	1.1365	0.0046	5.0993e-04
	3	114	1.1324	86170	88612	106119	107341	114.3647	1.1360	0.0046	9.7771e-04
1.362	1	137	1.3609	5183	7622	24306	26851	137.3311	1.3606	0.0011	-0.0022
	2	137	1.3609	45267	47709	64192	66634	137.2799	1.3632	0.0011	-0.0016
	3	137	1.3609	85458	87798	104183	106628	137.2388	1.3636	0.0011	-0.0012
1.875	1	188	1.8675	5284	7521	26137	28579	188.6231	1.8737	0.0075	4.4523e-04
	2	188	1.8675	44758	47097	65615	67854	188.6725	1.8741	0.0075	8.5307e-04
	3	188	1.8675	84642	87085	105504	107847	188.6662	1.8741	0.0075	9.1585e-04

continuous four sampling points is calculated as one sampling point. The experiment collected three sets of voltage data, each set contains three periods, the results are shown in Table 1.

5 Discussion

According to the equations (4) and (5), the solution procedure of the amplitude of the signal s has nothing to do with the start time t_1 of the saw-tooth wave, and is independent of the end of the forward and reverse saw-tooth waves. So this procedure avoids the error caused by the ΔN which has been introduced because the saw-tooth wave amplitude is not equal to integer multiple of LSB in the actual case in equation (1).

The error calculated by the readings of the ADC is determined by ΔS. When ΔS is small enough, the error is very small and the second set of data is in this case. Nevertheless, this is just a random situation, not universal. From all the experimental results, our method can effectively improve the measurement accuracy of the ADC and break through its maximum limitation. In order to make the calculated results more stable and reliable, we can figure the average of measuring results of multiple periods.

The error of affecting the accuracy of the signal s in the paper, which has been caused by bidirectional saw-tooth shaped function, is mainly from three aspects. The first is the accuracy of the t_3 and t_4 when signal amplitude of the forward saw-tooth wave is S + 2 in the first time and the last time. The second is the accuracy of the t_7 and t_8 when signal amplitude of the reverse saw-tooth wave is S-2 in the first time and the last time. That is, the higher the sampling frequency is in each LSB of the ADC, the more accurate the measurement time is, and the more accurate the calculated original signal value is. The third is the random noise and the jitter amplitude of the mixed signal.

6 Conclusion

In this paper, an innovative method has been developed, which makes it possible to use a lower-resolution ADC at a lower cost in a wearable device to detect weak signals. Compared to the traditional method of superimposing unidirectional saw-tooth wave, this new method can effectively solve the nonlinear problem of the starting point of the saw-tooth wave and eliminate the error caused by the fact that it is difficult for the amplitude of the saw-tooth wave to precisely control the integer multiple of the LSB. The new method for bidirectional saw-tooth waves only requires one stable linear interval greater than a complete LSB duration. Experiments show that our scheme improves the ADC resolution effectively. Our future work will focus on how to further improve the accuracy of the measurement.

Acknowledgements This work has been supported by National Natural Science Foundation of China under grant project No.61370179.

References

1. Analog Devices Inc (2017) Low Power, 2-Channel 24-Bit Sigma-Delta ADC. Data Sheets. http://www.analog.com/media/en/technical-documentation/data-sheets/AD7787.pdf
2. Chen M, Ma YJ, Li Y, Wu D, Zhang Y, Youn CH (2017) Wearable 2.0: Enable Human-Cloud Integration in Next Generation Healthcare System. IEEE Communications 55(1):54–61
3. Chen M, Shi X, Zhang Y, Wu D, Guizani M (2017) Deep Features Learning for Medical Image Analysis with Convolutional Autoencoder Neural Network. IEEE Transactions on Big Data. https://doi.org/10.1109/TBDATA.2017.2717439
4. Cheng X (2013) Design and implementation of continuous glucose monitoring system based on wireless. Dissertation, Huazhong University of Science and Technology
5. Kim JM, Kwon KH (2007) Recovery of finite missing samples in two-channel oversampling. Sampling Theory in Signal and Image Processing 6(2):185–198
6. Li G, Zhang L (2008) Weak Signal Detection Based on Over-Sampling and Saw-Tooth Shaped Function. Acta Electron Sin 36(4):756–759
7. Li H, Zhao F (2015) High Resolution and Wide Dynamic Range Infrasound Signal Acquisition System Based on Oversampling Techniques. Intstrument Technique and Sensor 5:62–64
8. Li G, Liu J, Li X et al (2014) A Multiple Biomedical Signals Synchronous Acquisition Circuit Based on Over-Sampling and Shaped Signal for the Application of the Ubiquitous Health Care. Circuits Systems and Signal Processing 33(10):3003–3017
9 Xu W, Wang J, Chen T (2007) Application of oversampling technique in the design of FOG data collection. Control & Measurement 3:75–76
10 Zhang Y, Chen M et al (2017) SOVCAN: Safety-Oriented Vehicular Controller Area Network. IEEE Communications 55(8):94–99
11 Zhang Y, Chen M, Huang DJ, Wu D, Li Y (2017) iDoctor: Personalized and Professionalized Medical Recommendations Based on Hybrid Matrix Factorization. Futur Gener Comput Syst 66:30–35
12 Zhang Y, Qiu MK, Tsai CW, Hassan MM, Alamri A (2017) Health-CPS: Healthcare Cyber-Physical System Assisted by Cloud and Big Data. IEEE Syst J 11(1):88–95

Enmin Song received his Ph.D. degree in Electrical Engineering and Computer from the Teesside University, UK. After completing his Ph.D, he was postdoctoral researcher at University Of California San Francisco (UCSF). He is a senior member of IEEE. He is currently a Professor at School of Computer Science and Technology, Huazhong University of Science and Technology, China. His current research interests involve medical image processing and medical image information analysis.

Ning Cheng received his Master degree in Computer Technology from Wuhan University of Technology of Wuhan. He is now a Ph.D. Student in Computer Application at Huazhong University of Science and Technology of Wuhan. His current research interests involve medical image processing and biological signal detection.

Hong Liu received her Ph.D. degree in Electrical Engineering and Computer from the Teesside University, UK. She is currently a Professor at School of Computer Science and Technology, Huazhong University of Science and Technology, China. Her current research interests involve medical image processing, pattern recognition and algorithmic design and analysis.

Huimin Song received his Ph.D. degree in Applied Science from South Bank University, UK. He is working as an Electrical Engineer and Programmer in Central City Brewers and Distillers, Canada. His current research and interests are Robot Automation and Process Controller.